Postprint of: Pladzyk A., Hnatejko Z., Baranowska K., Binuclear Co(II), Zn(II) and Cd(II) tri-tert-butoxysilanethiolates. Synthesis, crystal structure and spectroscopic studies, Polyhedron, Vol. 79 (2014), pp. 116-123, DOI: 10.1016/j.poly.2014.04.049

Binuclear Co(II), Zn(II) and Cd(II) tri-*tert*-butoxysilanethiolates. Synthesis, crystal structure and spectroscopic studies.

Agnieszka Pladzyk*[a], Zbigniew Hnatejko[b], Katarzyna Baranowska[a]

[a] *Department of Inorganic Chemistry, Chemical Faculty, Gdańsk University of Technology Narutowicza Str. 11/12, 80-233 Gdańsk, Poland*

[b] *Faculty of Chemistry, Adam Mickiewicz University, Umultowska 89b, 61-414 Poznań, Poland*

* Corresponding author. *e-mail address*: agnieszka.pladzyk@pg.gda.pl (A. Pladzyk), tel.: +48 583472329; fax.: +48 583472694.

Abstract

A series of Co(II), Zn(II) and Cd(II) complexes have been synthesized in reaction of respective metal tri-*tert*-butoxysilanethiolates with pyrazine **1**-**2** and 1,2-bis(2-pyridyl)ethylene **3**-**5**. All compounds have been characterized by single-crystal X-ray structure determination, elemental analysis, FT-IR and thermogravimetry. Obtained complexes are bimetallic with the formula of $[M\{SSi(OtBu)_3\}_2(\mu\text{-}L)]_2$ and metal ions bridged by N,N'-spacer. The penta-coordinated spheres of the metallic atoms are completed by tri-*tert*-butoxysilanethiolate residue playing the role of O,S-chelating ligand. Luminescent properties of **1**, **2**, **4** and **5** complexes have also been investigated in solid state.

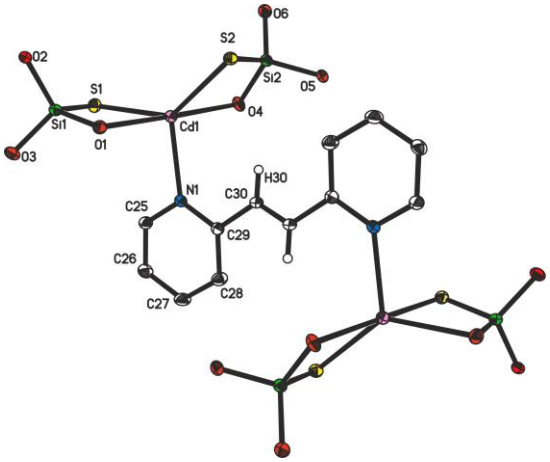

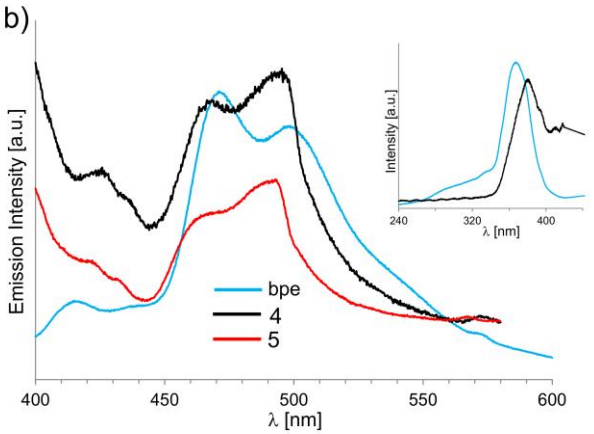

Keywords: Binuclear complexes; Bridging ligands, Tri-*tert*-butoxysilanethiol; Crystal structures; Spectroscopic analysis; Luminescence.

1. Introduction

The construction of organic-inorganic hybrid materials based on covalent interaction is the area of constant development and the rigid rod-like spacer molecules like bipyridines have been useful in building blocks for their construction serving as super-exchange lanes between metal ions [1]. This group of ligands is capable of mediating in intermetallic electronic communications through the π-symmetry orbitals and is also useful in synthesis of dinuclear complexes which exhibit chemical features, like magnetization, catalysis, conductivity or luminescence [2].

Up to now, though a number of such complexes with transition metal have been described, the design and construction of new compounds with new type of ligands is still a

challenge. Our longstanding interest in the sulfur containing compounds *e.g.* thiolates has arisen from their fascinating properties. They have been used in synthesis of small molecule analogues of metal-containing active sites of metalloproteins as well as in syntheses of coordination polymers [3,4]. They can also serve as candidates as "single-source" precursors for metal sulfide materials [5].

As the part of our work concerning design and preparation of functional multicenter complexes, we have carried out the synthesis of transition metal compounds with mixed ligand system of tri-*tert*-butoxysilanethiol $(tBuO)_3SiSH$ and bridging N-ligands [6-9]. Tri-*tert*-butoxysilanethiol itself is relatively stable in atmospheric conditions [10] and has been found to be a multi-tasking ligand, which can act as S-monodentate, S-bridging, as well as O,S-chelating ligand in mono- and polymetallic compounds [6-9,11-14].

In the chemistry of Co, Zn and Cd there are many examples of complexes in which metal ions are held together by a pyrazine and bypiridine-like bridging ligands. Among them there are some examples that contain additional S-donor ligands but the coordination sphere of metal ions is completed by dithiophosphate [15], dithiocarbamate [16] or dithiolate derivatives [17]. There are only three zinc complexes described by Vittal *et all.* that contain thiolate residue as additional ligands and metallic centers bridged by 4,4'-bipyridine [18].

Among complexes synthesized by us so far, we have obtained some dinuclear Cd(II), Zn(II) and Co(II) silanethiolates with 4,4'-bypiridine and $[Co_2\{SSi(OtBu)_3\}_4(\mu\text{-}C_4H_4N_2)]$ with pyrazine [6-9]. Our last investigations have concerned further introduction of pyrazine (pz) and new ligand 1,2-bis(2-pyridyl)ethylene (bpe) into the Co(II), Cd(II) and Zn(II) silanethiolates. Admittedly both molecules can act as monodentate or μ_2-bridging ligands but bpe ensure larger distance between metal ions than pyrazine and may act as flexible ligand due to the presence of a –CH=CH– spacer between pyridine ring, allowing for their bending and rotation. Here we report syntheses and structures of five new binuclear complexes $[M_2\{SSi(OtBu)_3\}_4(\mu\text{-pz})]$ (**1** Zn, **2** Cd) and $[M_2\{SSi(OtBu)_3\}_4(\mu\text{-bpe})]$ (**3** Co, **4** Zn, **5** Cd), the comparison of metal coordination geometry, thermal and photoluminescence properties.

2. Experimental

2.1. General procedures

The elemental analyses (C, H, S and N contents) were performed on an Elemental Analyser EA 1108 (Carlo Erba Instruments). The IR spectra were measured for crystalline compounds in the range of 4,000 - 700 cm^{-1} with a Momentμm microscope (IR detector)

attached to a Mattson Genesis II Gold spectrometer (IR source). Luminescence characterizations were performed on a Hitachi F-7000 fluorescence spectrophotometer equipped with a xenon lamp (150 W) as the light source for steady state measurement (emission and excitation spectra measurement). For accuracy of data, the solid state samples were measured within the same sample holder to ensure the consistent amount of luminescent materials in all samples. Excitation and emission spectra were corrected for the instrumental response. All measurements were carried out under the same experimental conditions. Diffuse reflectance spectra were recorded on a Varian Cary 100 UV-Vis Spectrophotometer with DRA-CA-301 Diffuse Reflectance Accessory.

2.2. Syntheses

Tri-*tert*-butoxysilanethiol, $[Co\{SSi(OtBu)_3\}_2(NH_3)]_2$ and $[Cd\{SSi(OtBu)_3\}_2]_2$ were obtained according to procedures described previously [10,19,20]. All other reagents were obtained commercially.

2.2.1. $[Zn_2\{SSi(OtBu)_3\}_4(\mu\text{-}C_4H_4N_2)]$ ***1***

The $Zn(acac)_2$ (0.6 mmol, 0.16 g) was dissolved in acetonitrile (5 mL) and tri-*tert*-butoxysilanethiol (1.2 mmol, 0.4 mL) was added dropwise. Simultaneously pyrazine (0.06 mmol, 0.05 g) was dissolved in acetonitrile (2 mL) and added to the solution. Compound **1** crystallizes immediately after mixing the reagents as colorless crystals. *Anal*. Calc. for $C_{52}H_{112}N_2O_{12}S_4Si_4Zn_2$ (1328.86): C, 47.00; H, 8.50; N, 2.11; S, 9.65. Found C, 47.01; H, 8.49; N, 2.15; S, 9.68%.M. p. 246-247 °C. IR (solid state): ν = 3108 (w), 3027 (w), 2976 (vs), 2934 (vs), 2915 (s), 2876 (s), 1473 (s), 1427 (s), 1390 (vs), 1365 (vs), 1243 (vs), 1203 (vs, br), 1187 (vs), 1132 (s), 1051 (vs, br), 1028 (vs), 995 (vs), 963 (vs), 918 (m), 822 (s), 804 (w), 774 (w) cm^{-1}.

2.2.2. $[Cd_2\{SSi(OtBu)_3\}_4(\mu\text{-}C_4H_4N_2)]$ ***2***

$[Cd\{SSi(OtBu)_3\}_2]_2$ (0.1 mmol, 0.13 g) and pyrazine (0.03 g, 0.4 mmol) were separately dissolved in methanol (5 mL) and mixed. The reaction flask was left at 8 °C for two months and some colorless crystals of complex **2** were received. *Anal*. Calc. for $C_{52}H_{112}S_4Si_4O_{12}N_2Cd_2$: C 43.89; H, 7.93; S, 9.01; N, 1.97%. Found: C 43.83; H, 7.82; S, 9.01; N, 1.98%. M. p. 196-198 °C. IR (solid state): ν = 3100 (w), 3027 (w), 2982 (vs), 2932 (vs), 2910 (s), 2875 (s), 1472 (s), 1466 (s), 1424 (s), 1389 (vs), 1365 (vs), 1244 (vs), 1205 (vs, br),

1195 (vs), 1160 (s), 1131 (s), 1060 (vs, br), 1028 (vs), 992 (vs), 976 (vs), 915 (m), 822 (s), 803 (w), 796 (w), 770 (m) cm^{-1}.

*2.2.3. [Co_2{SSi(OtBu)$_3$}$_4$(μ-$C_{12}H_{10}N_2$)] **3***

[Co{SSi(OtBu)$_3$}$_2$(NH_3)]$_2$ (0.1 mmol, 0.13g) in methanol (10 mL) was mixed with bpe (0,1 mmol, 0,02 g) dissolved in methanol (2 mL). Compound **3** crystallizes immediately after few minutes as pink-violet crystals. *Anal*. Calc. for $C_{60}H_{118}N_2O_{12}S_4Si_4Co_2$ (1418.07): C, 50.82; H, 8.38; N, 1.97; S, 9.04. Found C, 50.89; H, 8.41; N, 2.01; S, 9,03%. M. p. at 253-256 °C. IR (solid state): ν = 3104 (w), 3024 (w), 2976 (vs), 2932 (vs), 2915 (s), 2877 (s), 1744 (w), 1603 (s), 1563 (s), 1489 (s), 1473 (s), 1442 (s), 1388 (vs), 1364 (vs), 1343 (m), 1293 (w), 1240 (vs), 1204 (vs, br), 1189 (vs), 1100 (w), 1060 (vs, br), 1043 (vs), 1024 (vs), 970 (vs), 914 (m), 821 (vs), 802 (s), 788 (s), 756 (w) cm^{-1}.

*2.2.4. [Zn_2{SSi(OtBu)$_3$}$_4$(μ-$C_{12}H_{10}N_2$)] **4***

(tBuO)$_3$SiSH (1.2 mmol, 0.4 mL) was added to a solution of Zn(acac)$_2$ (0.6 mmol, 0.16 g) in CH_3CN (15 mL). Obtained solution was limpid and colorless. Next, $C_{12}H_{10}N_2$ (0.4 mmol, 0,08 g) in CH_3CN (5 mL) was added to the previous solution. After gentle stirring for a few minutes, the mixture was allowed to stand at 4°C to yield colorless crystals of the complex **4**. *Anal*. Calc. for $C_{60}H_{118}N_2O_{12}S_4Si_4Zn_2$ (1430.98): C, 50.36; H, 8.31; N, 1.95; S, 8.96. Found C, 49.96; H, 8.25; N, 1.94; S, 8.96%. M. p. at 253-255 °C. IR (solid state): ν = 3122 (w), 3024 (w), 2976 (vs), 2933 (vs), 2882 (s), 2850 (w), 1606 (s), 1570 (s), 1488 (s), 1474 (s), 1445 (s), 1389 (vs), 1290 (w), 1242 (vs), 1206 (vs, br), 1189 (vs), 1123 (w), 1101 (w), 1047 (vs), 1023 (vs), 984 (vs), 914 (w), 823 (vs), 803 (s), 789 (s), 758 (w) cm^{-1}.

*2.2.5. [Cd_2{SSi(OtBu)$_3$}$_4$(μ-$C_{12}H_{10}N_2$)] **5***

[Cd{SSi(OtBu)$_3$}$_2$]$_2$ (0.1 mmol, 0.13 g) suspended in ethanol (5 mL) was mixed with $C_{12}H_{10}N_2$ (0.1 mmol, 0.02 g) dissolved in toluene (5 mL). The mixture was stirred until the solution became to be limpid. After crystallization at 4°C colourless crystals of **5** were obtained after a few days. *Anal*. Calc. for $C_{60}H_{118}N_2O_{12}S_4Si_4Cd_2$ (1525.03): C, 47.25; H, 7.79; N, 1.84; S, 8.41. Found C, 47.31; H, 7.83; N, 1.78; S, 8.39%. M. p. at 205-206 °C. IR (solid state): ν = 3102 (w), 3018 (w), 2977 (vs), 2932 (vs), 2916 (s), 2875 (s), 1747 (w), 1681 (w), 1600 (s), 1567 (s), 1491 (s), 1473 (s), 1440 (s), 1389 (vs), 1363 (vs), 1343 (w), 1291 (w),

1240 (vs), 1204 (vs, br), 1186 (vs), 1167 (vs), 1131 (s), 1097 (m), 1060 (vs, br), 1049 (vs), 977 (vs), 913 (m), 821 (s), 802 (w), 791 (w), 754 (m), 737 (m) cm^{-1}.

2.3. X-ray crystallography

Diffraction data were recorded on a KUMA KM4 diffractometer with graphite-monochromated MoKα radiation, equipped with Sapphire 2 CCD detector (Oxford Diffraction). The apparatus was equipped with an open flow thermostat (Oxford Cryosystems), which enabled experiments at 120 K. The structures were solved with direct methods and refined with the SHELX-97, program package [21] with the full-matrix least-squares refinement based on F^2. Hydrogen atoms were refined using isotropic model with *Uiso*(H) values fixed to be 1.5 times *Ueq* of C atoms for CH_3 or 1.2 times *Ueq* for CH groups. Hydrogen atoms H30a in complexes **3-5** were found in the electron density Fourier map and refined without constraints. Disordered tBu groups: C14-C16 in **1** (*s.o.f.* 0.593(8)/0.407(8)); in **2** C3-C4 (*s.o.f.* 0.487(8)/0.513(8)); C11-C12 (*s.o.f.* 0.68(4)/0.32(4)) and C18-C20 (*s.o.f.* 0.625(8)/0.375(8)). Basic crystal data, description of the diffraction experiment, and details of the structure refinement are given in Table 1.

Table 1 Crystallographic data and structure refinement details.

3. Results and Discussion

*3.1. Synthesis and spectral characterization of **1-5***

We have investigated the bridging properties of pyrazine (pz) and 1,2-bis(2-pyridyl)ethylene (bpe) used in reactions with Co (II), Cd(II) and Zn(II) tri-*tert*-butoxysilanethiolates. As a result, we have obtained complexes **1**-**5** prepared as single crystal products and formulated as dinuclear compounds (Scheme 1).

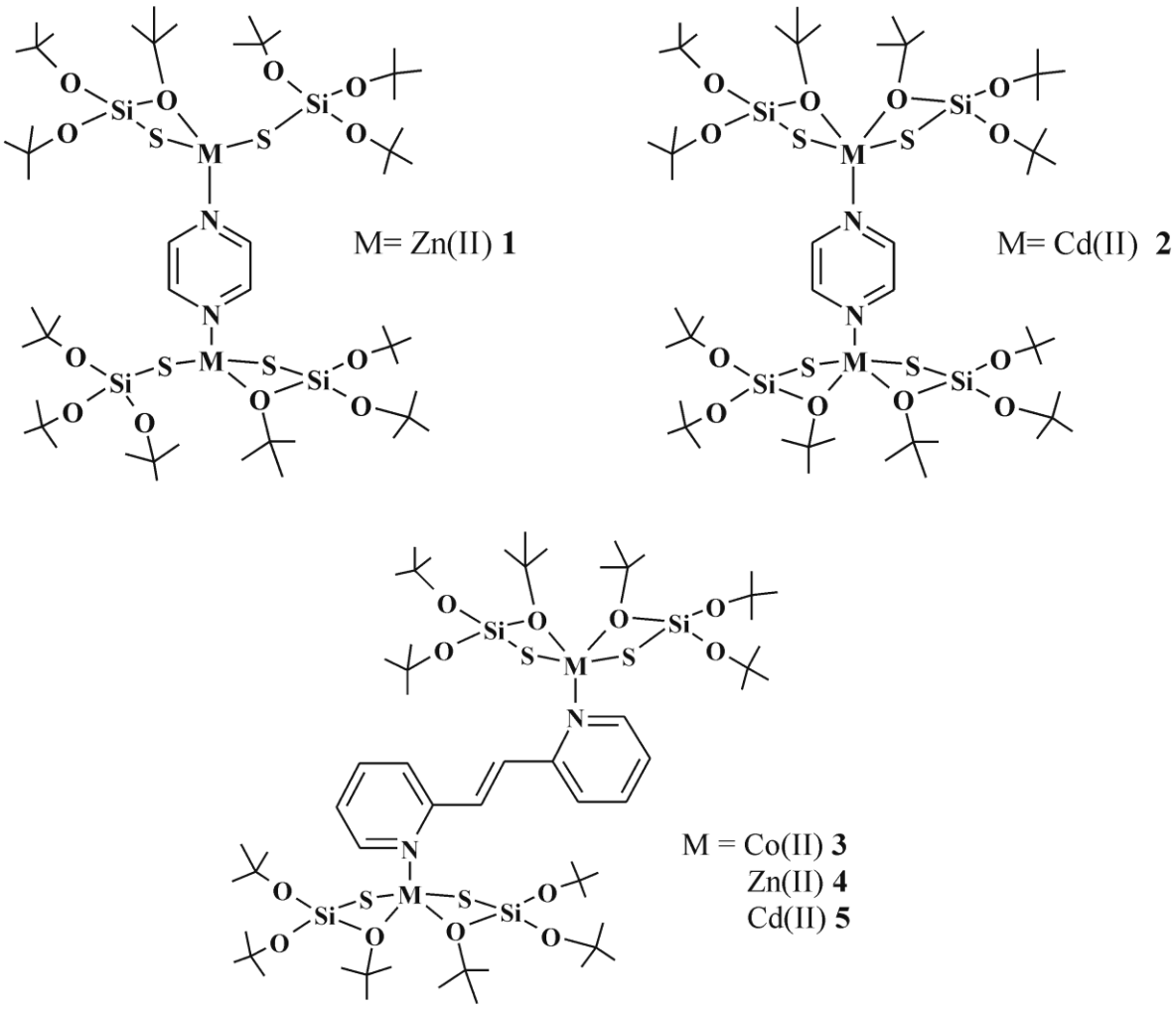

Scheme 1 Obtained complexes **1**-**5**.

As a first, we combined equimolar amounts of Zn ions, tri-*tert*-butoxysilanethiol and pyrazine at room temperature in acetonitrile. The reaction run very rapidly to form a colorless crystals of $[Zn_2\{SSi(OtBu)_3\}_4(\mu\text{-}C_4H_4N_2)]$ **1**. The reaction of $[Cd\{SSi(OtBu)_3\}_2]_2$ and pyrazine in methanol also yielded colorless crystals of $[Cd_2\{SSi(OtBu)_3\}_4(\mu\text{-}C_4H_4N_2)]$ **2** but the crystallization process lasted two month at low temperature. Complexes **1** and **2** are isomorphous and contain metal ions coordinated by two sulfur atoms from two silanethiolate residues and one nitrogen atom from bridging ligand molecule. The arrangement of the ligands around the metal atoms facilitates the formation of additional interactions of two siloxy oxygen atoms and results in an $ZnNOS_2$ and $CdNO_2S_2$ core in **1** and **2**, respectively.

The synthetic procedure described above was also applied in the synthesis of next three bimetallic complexes **3**-**5** with formula of $[M_2\{SSi(OtBu)_3\}_4(\mu\text{-bpe})]$ (M = Co **3**, Zn **4**, Cd **5**) with bpe as the bridging ligand.

It is noteworthy that binuclear complexes **1-5** were formed even in cases when the stoichiometry of reactions was designed to isolate polymeric species. This behavior could be related to the reduced solubility of the binuclear species and/or steric effects of used ligands.

The vibrational spectra recorded for solid **1-5** (700–3700cm^{-1}) were in agreement with their formulations [22] (Figure S1 Supplementary Materials). Sharp weak intensity bands in the range of 3095 cm^{-1} to 3099 cm^{-1} were ascribed to stretching modes of C–H bond of the phenyl ring moiety. In metal silanethiolates, where oxygen from Si–O–tBu residue interacts with the metal atom, a broad band in the range of 950-990 cm^{-1} is observed [11-14]. Admittedly all compounds contain M–O–tBu bonds, but a detailed analysis of the vibrational spectra revealed some subtle differences in this region.

*3.2. Description of Structures of **1** and **2***

Compounds **1** and **2** are packed as discrete entities with no other than van der Waals interactions. Both complexes are centrosymmetric with the inversion center located in the midpoint of the pyrazine ring as it is present in isostructural $[Co_2\{SSi(OtBu)_3\}_4(\mu\text{-}C_4H_4N_2)]$ [8]. Figures 1 and 2 gives a view of complexes **1** and **2** with atom labeling scheme. The selected bond lengths and angles are listed in Table 2.

Table 2 Selected interatomic distances (Å) and angles (°) for **1** and **2**.

In order to estimate the geometric shape of obtained complexes, the Addison angular structural parameter (τ) has been calculated [23]. The τ_4 and τ_5 parameters for four- and five-coordinate complexes are defined as $\tau_4 = [360° - (\alpha + \beta)]/141°$ and $\tau_5 = (\alpha - \beta)/60°$, where α and β are the largest bond angles in a complex. For complexes with coordination number CN = 5, τ_5 becomes unity for a perfectly trigonal bipyramidal geometry and $\tau_5 = 0$ for tetragonal pyramid. For four coordinated complexes perfectly square planar geometry $\tau_4 = 0$, while it becomes unity for a perfectly tetrahedral geometry.

The structure of complex **1** shows that one silanethiolate group acts as a bidentate *O,S*-ligand occupying two sites in coordination environments of Zn (O1 and S1) atom, whereas the second $SSi(OtBu)_3^-$ ligand appears only as monodentate ligand via S2 atom (Fig. 1 and Fig. S2 *Supplementary Materials*). The O1 and O4 atoms assume specific position around Zn ion and are distant from the metal ion on 2.271(2) and 2.710(2) Å, respectively. These values significantly exceed the sum of covalent radii of zinc and oxygen atoms (1.91 Å). However

the interaction between Zn and O1 atom is the shortest among all Zn–$O_{silanethiolate}$ bonds found in binuclear zinc silanethiolate [9] and in other mononuclear zinc silanethiolates containing bidentate $SSi(OtBu)_3^-$ residues, whereas between Zn and O4 is the longest one [9,11,13]. Therefore the Zn–O1 interaction can be considered as a virtual bond. Consequently, considering this complex structure as four coordinated the parameter τ_4 is 0.32 which points at four coordinated Zn ion with strongly distorted tetrahedral geometry. On the other hand, assuming that complex **1** is five-coordinated, the parameter τ_5 calculated is 0.57. The value is about halfway between a square pyramid and a trigonal bipyramid, although slightly closer to the latter, with the oxygen atoms occupying apical positions. To establish the ultimate geometry on Zn ions in complex **1** we turned our attention on the value of the S–Zn–S angle. Interestingly, in all Zn pentacoordinated silanethiolate complexes with a $ZnNO_2S_2$ kernel it ranges from 125.69(3) to 139.40(4) and decreases to 107.13(6)–120.35(3) in tetrahedral $ZnNOS_2$ and ZnN_2S_2 species [11,13,14]. The value of S1–Zn1–S2 in **1** is even wider (140.26(3)°), therefore we treat this parameter as the crucial one and consider complex **1** as penta-coordinated with strongly distorted trigonal bipyramidal NO_2S_2 geometry on Zn(II) ion. These deviations from ideal angles can be attributed to the need to accommodate the bulky silanethiolato groups effecting also the Zn–N bond distance (2.118(2) Å), which is longer than those found in other zinc silanethiolates with N-ligands synthesized so far, whereas Zn–S bond lengths (2.2577(9), 2.2276(9) Å) are slightly shorter. The plane formed by N1, N1A, Zn1 and Zn1A atoms shows significant rotation of pyrazine ring with C25 and C26 atoms located above and below the plane at 0.963 and 0.969 Å. The Zn···Zn distance is 7.0040(5) Å which indicates that the zinc atoms in **1** are not involved in metal-metal bonding interactions.

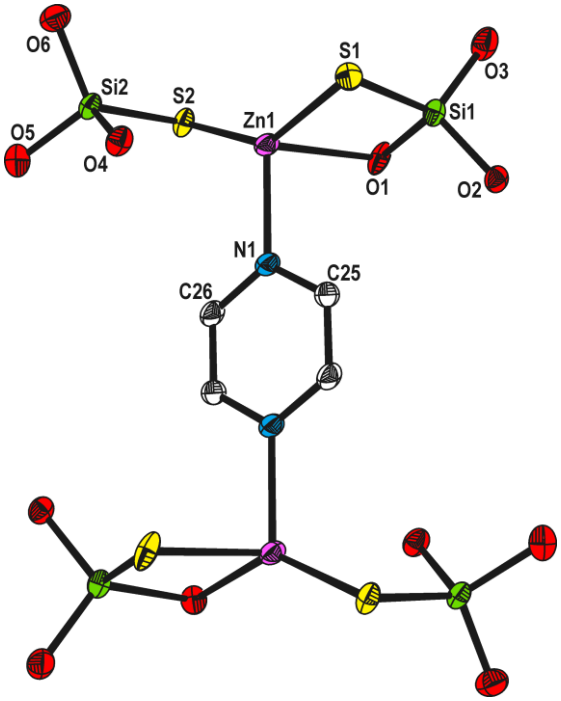

Fig. 1. Molecular structure of $[Zn_2\{SSi(OtBu)_3\}_4(\mu\text{-}C_4H_4N_2)]$ **1** with atom labeling scheme (tBu groups and hydrogen atoms of aromatic rings omitted for clarity). Thermal ellipsoids are drawn at 30% probability

The geometry of the coordinating atoms in complex **2** may be approximated to a square pyramidal (τ_5 = 0.39) with plane formed by atoms S1, S2 and O1 and O4 atoms and N1 atom in axial position (Fig. 2 and Fig. S3 *Supplementary Materials*). The distance between Cd1 and O1 and O4 atoms are 2.746(2) and 2.501(2) Å, respectively and the O1–Cd1–O4 angle value of 171.18(6)°. The Cd–O distances are longer than the sum of covalent radii of cadmium and oxygen atoms (2.15 Å) and even longer than the average Cd–O bond distance (2.36 Å). However, one of these two distances is shorter than those found in other cadmium silanethiolates [6,7,12-14]. Nevertheless both of them can be considered as weak covalent bonds. It is worth noting that the S1–Cd1–S2 angle is the widest (147.75(3)°) and Cd1–S1 and Cd1–S2 bond distances are relatively short (2.4106(9) and 2.4326(7) Å), which suggests strong interactions between cadmium and sulfur in **2**. Those values are comparable to Cd–S bond distances present in two binuclear cadmium silanethiolates obtained so far [6] and shorter than these found in other pentacoordinated cadmium silanethiolates containing chelating O,S-silanethiolate residues [13,14]. Complexation of O1 and O4 with cadmium does not influence on the Si–O bond distances: Si1–O1 and Si2–O4 are 1.656(2) Å. The plane formed by N1, N1A, Cd1 and Cd1A atoms shows small rotation of pyrazine ring with C49

and C50 atoms located above and below the plane at 0.491 and 0.493 Å. The Cd···Cd distance is 7.5566(4) Å which is only 0.5526 Å longer that the distance between Zn atoms in **1**.

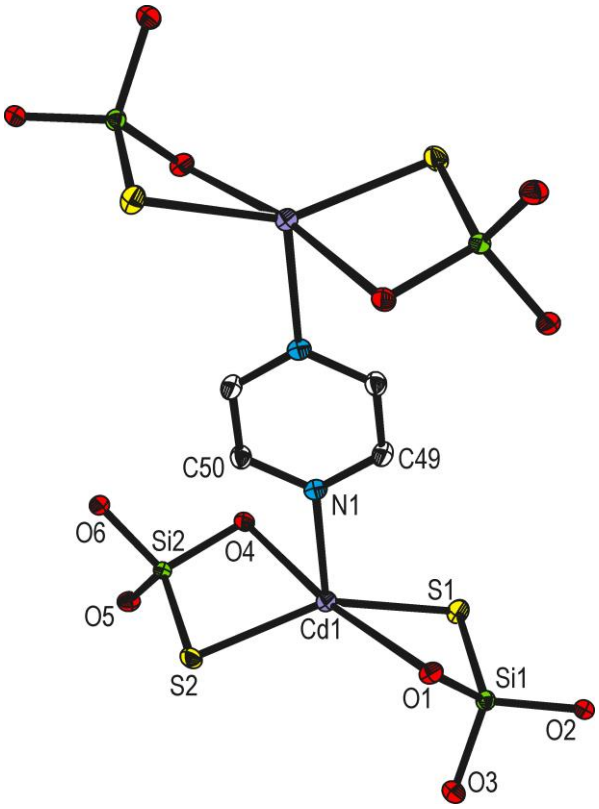

Fig. 2. Molecular structure of $[Cd_2\{SSi(OtBu)_3\}_4(\mu\text{-}C_4H_4N_2)]$ **2** with atom labeling scheme (tBu groups and hydrogen atoms of aromatic rings omitted for clarity). Thermal ellipsoids are drawn at 30% probability.

*3.3. Description of Structures of **3-5***

Crystal structures of **3-5** complexes contain a binuclear $[M\{SSi(OtBu)_3\}_2(\mu\text{-bpe})]_2$ (M = Co **3**, Zn **4**, Cd **5**). The selected bond angles and distances are given in Table 3. The view of **3** and **4** are given in Fig. 3 and Fig. S5 and their crystal packing in Fig. S4 and S6 *Supplementary Materials*. Co(II) in **3** and Zn(II) in **4** are penta-coordinated and display a strongly distorted trigonal bipyramidal coordination environment due to the geometric parameter τ_5 (0.72 and 0.75, respectively). Both complexes have inversion centers located at the mid-point of the bridging C30–C30A bond between pyridyl rings of the bpe ligand, at Wyckoff position *c* $(0,\frac{1}{2},0)$ in **3** and *d* $(\frac{1}{2},0,0)$ in **4**. Closer look into structures of **3** and **4**

showed that bpe rings are not coplanar - one pyridyl ring lies int the $CoNS_2$ plane, whereas the second one is placed below this plane at the distance in the range of 0.481-0.532 Å. These deviations are even stronger in complex **4** (0.216 - 1.024).

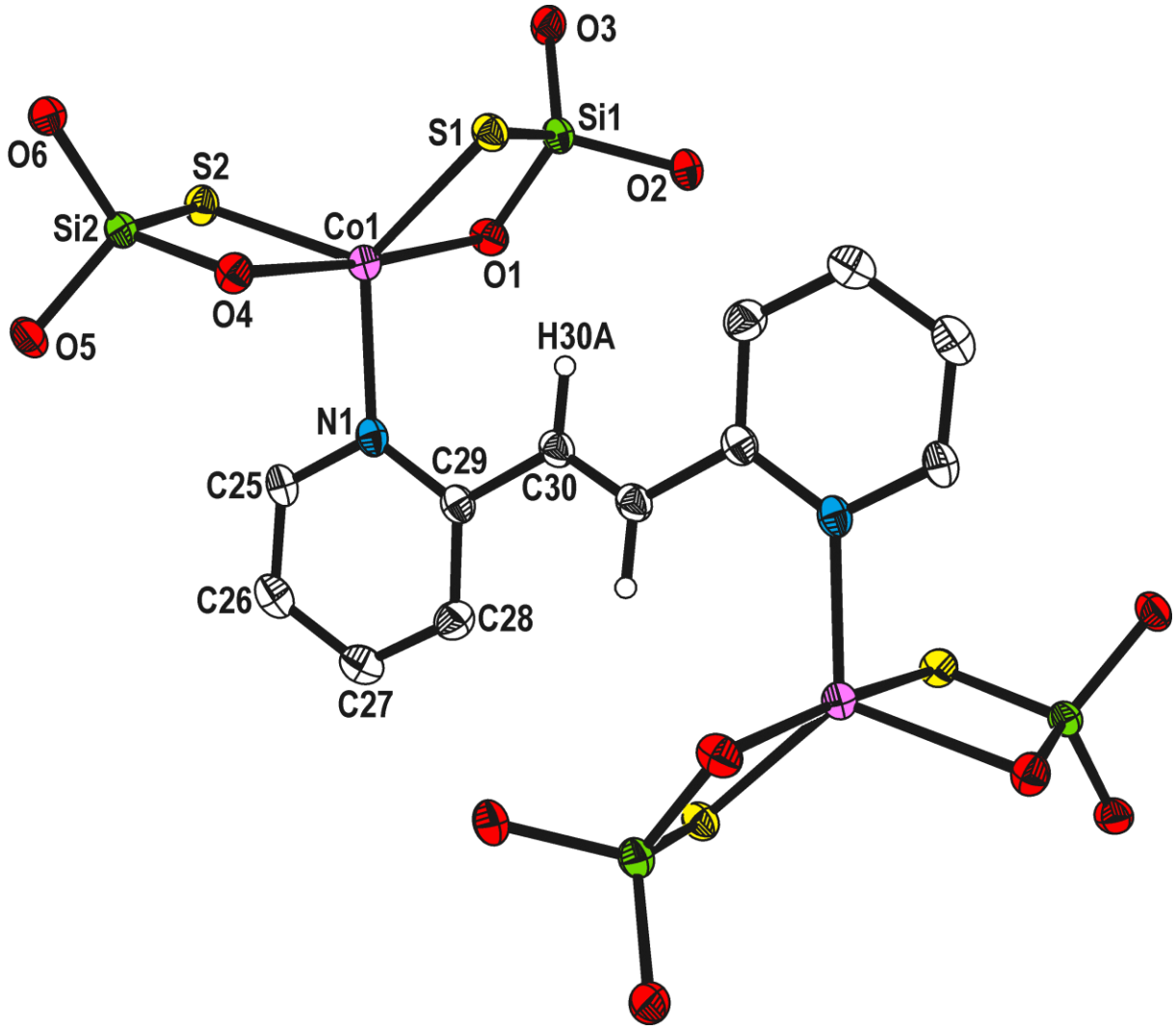

Fig. 3. Molecular structure of $[Co_2\{SSi(OtBu)_3\}_4(\mu\text{-}C_{12}H_{10}N_2)]$ **3** with atom labeling scheme (tBu groups and hydrogen atoms of aromatic rings omitted for clarity). Thermal ellipsoids are drawn at 30% probability.

The Co–O distances in **3** are 2.350(2) Å and 2.340(2) Å, which are longer than the sum of the covalent radii of cobalt and oxygen, but shorter than Co–O distances present in binuclear $[Co_2\{SSi(OtBu)_3\}_2]_4(\mu\text{-}4,4'\text{-bipy})]$ complex with penta-coordinated Co atoms. The O1–Co1–O4 and the S1–Co1–S2 angles in **3** ((174.03(8)° and 120.66(4)° respectively) are also wider than the respective angles found in $[Co_2\{SSi(OtBu)_3\}_2]_4(\mu\text{-}4,4'\text{-bipy})]$ [8]. The same type of interactions is present in complex **4** between Zn1 and O1 and O4 atoms (2.400(2) and 2.481(3) Å). These distance values are in the range of Zn-$O_{silanethiol}$ bond distances (2.271(2)-2.5832(19) Å) present in other zinc silanethiolates with Zn chelated by

two $(tBuO)_3SiS^-$ ligands and also in binuclear $[Zn_2\{SSi(OtBu)_3\}_4(\mu\text{-}4,4'\text{-bipy})(CH_4O)]$ synthesized so far [9]. The comparison of bond lengths and angles within metallic centers of **3** and **4** shows that related parameters stick out of those found in binuclear Co and Zn silanethiolates previously published [8,9]. Admittedly the Co–S, Co–N, S–Si and Si–O bond lengths are only slightly longer in complex **3** when compare with $[Co_2\{SSi(OtBu)_3\}_2]_4(\mu\text{-}4,4'\text{-bipy})$) [8], but the differences are better seen in the case of zinc complex **4** in comparison with complex $[Zn_2\{SSi(OtBu)_3\}_4(\mu\text{-}4,4'\text{-bipy})(CH_4O)]$ [9]. Nevertheless the Metal···Metal distances are comparable and vary from 7.7490(8) Å in complex **3** to 7.6929(5) Å in complex **4**.

Complex **5** is also isostructural with **3** and **4** complexes. (Fig. S7 and S8 *Supplementary Materials*). The specific spatial arrangement of the ligands around Cd ions facilitate the formation of two additional Cd(1)–O(1) and Cd(1)–O(4) interactions equal to 2.520(2) and 2.528(2) Å, respectively and O(1)–Cd(1)–O(4) angle with the value of 176.55(6)°, which is the widest among O(1)–M(1)–O(4) angles present in **1-5** complexes. Nevertheless the interactions are shorter than the analogous interactions present in complex **2** and binuclear $[Cd_2\{SSi(OtBu)_3\}_2]_4(\mu\text{-}4,4'\text{-bipy})\cdot 2C_7H_8]$ (2.5137(13) and 2.5384(13) Å) and it's THF disolvate analogue (2.552(2) Å and 2.577(2) Å) [6], therefore we considered them as covalent bonds. As a result, the coordination sphere of the Cd(1) ions are $CdNO_2S_2$. Consequently, the environment of the Cd atoms can be approximated to trigonal-bipyramidal (τ_5=0.71). Geometrical distortion from ideal angles can be attributed to the need to accommodate the bulky silanethiolato groups. The Cd–S, Cd–O and Cd-N bond lengths are found in good agreement with within the expected ranges (Cambridge Structural Database, Version 5). The value of S(2)–Cd(1)–S(1) bond angle is 134.03(2) and is narrower than the analogous angle in binuclear Cd silanethiolates mentioned above [6]. Also, an inversion center is located at the mid-point of the bridging C30–C30A bond of the bpe, at Wyckoff position *b* $(\frac{1}{2},\frac{1}{2},\frac{1}{2})$. The bpe rings are almost parallel and one pyridyl ring lies in the $CdNS_2$ plane, whereas the second one exhibits deviation from this plane n the range of 0.126-0.723 Å. The Cd···Cd distance is 8.1445(4) Å

Table 3 Selected interatomic distances (Å) and angles (°) for **3-5**.

3.4. Luminescence

The spectroscopically studied compounds are transparent materials in the visible wavelengths (Fig. 4). Taking into account that the d^{10} metal ions complexes often exhibit luminescence [24-26] the studied solid complexes have been examined, at room temperature, from the point of view of their emission characteristics, as shown in Fig. 5.

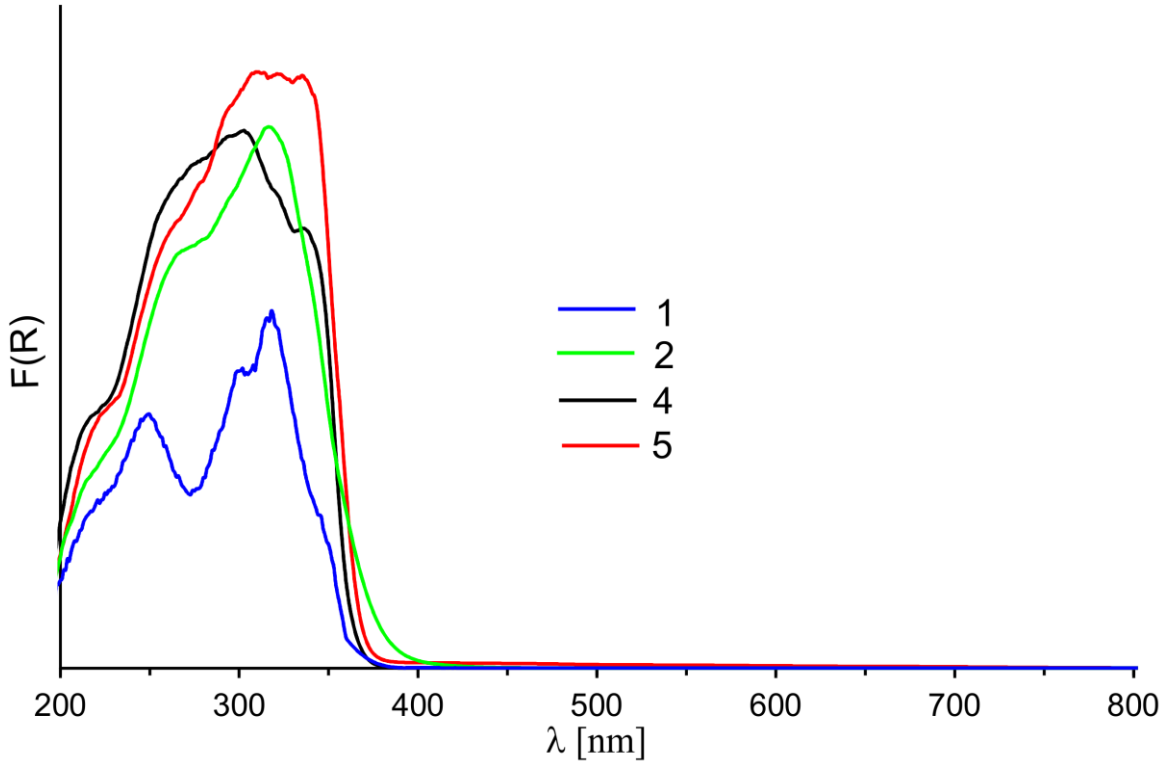

Fig. 4. Diffuse reflectance spectra of obtained compounds **1**, **2**, **4** and **5**.

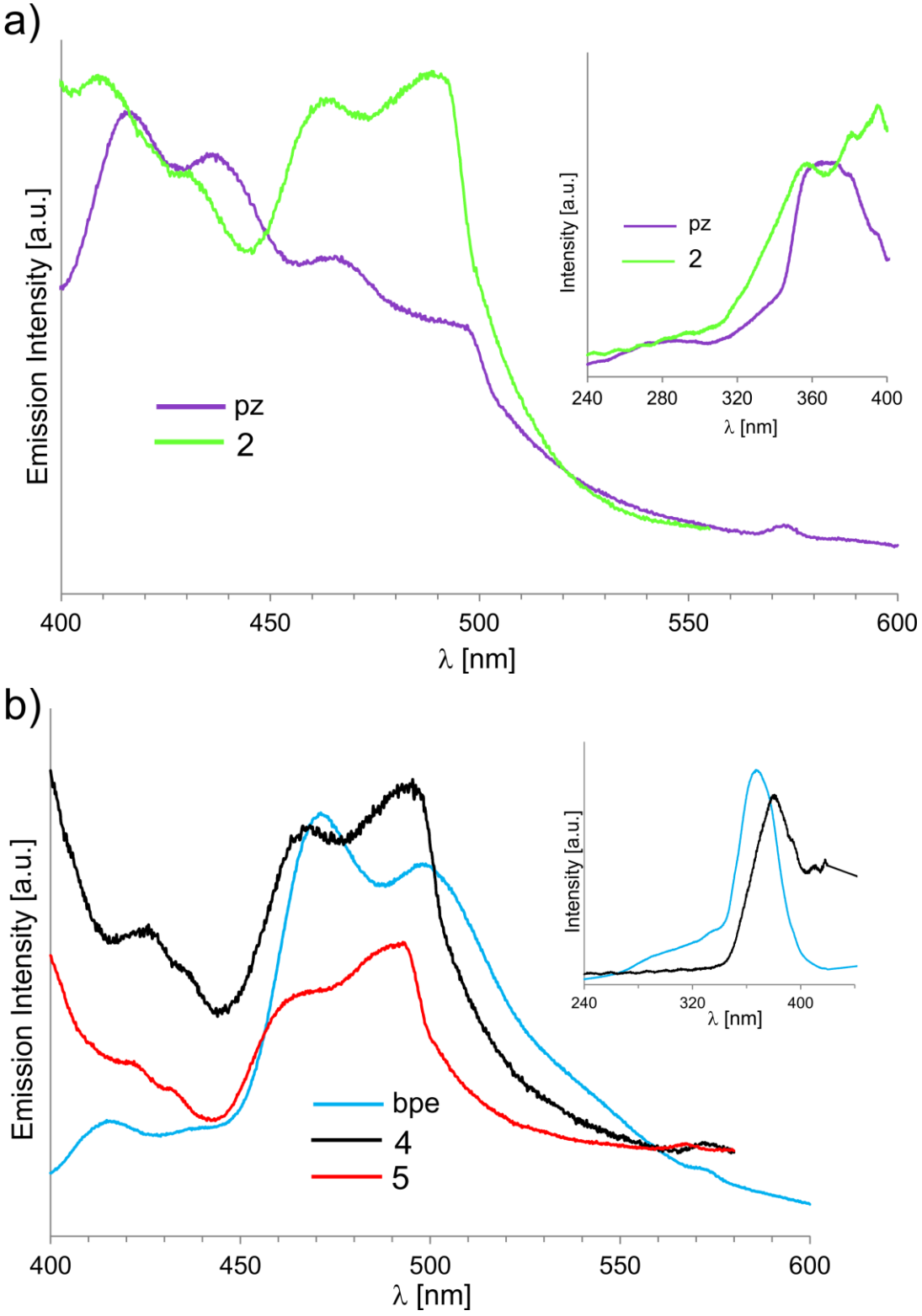

Fig. 5. Photoluminescent spectra: (a) of pz ligand and complex **2** and (b) bpe ligand and complexes **4-5** in the solid state at room temperature; the inset are the excitation spectra of all studied systems.

The main chromosphere of studied compounds are the aromatic six-membered pyrazine and pyridine rings. Free pyrazine ligand exhibit unsymmetrical emission with four bands at λ=416, 436, 468 and 494 nm upon photoexcitation at λ=380 nm (Fig.5a). The corresponding complexes **1** and **2** show emission bands at the same wavelengths when were excitated at λ=380 nm. Compared with free pz ligand, complexes showed the increase intense bands at λ=468 and 494 nm. Moreover the emission intensity of both complexes was similar (hence, in Fig.5a is shown only the spectrum of complex **2**). Since the shapes of the emission spectra of both complexes are similar to that of pz, luminescence emission bands, observed in these complexes, may be assigned to intraligand interactions.

The emission spectra of compounds **4** and **5** present emissions at about 465 and 493 nm (λ_{ex}=380 nm, Fig.5b). The emission bands are blue-shifted compared to the corresponding ligand bpe (λ=471 and 499 nm). This effect indicates that the luminescence emission, in these compounds, may be due to the metal-to ligand charge transfer (MLCT) [27-30] or may be resulted from intraligand transitions (the shifts may be assigned to the ligand chelating or bridging effect due to the coordination of M^{2+} ions) [31,32]. Above all, obtained results show that complexes **1**, **2** and **4**, **5** may be candidates for potential photoactive materials.

3.5. Thermal analysis

Different techniques of thermal analysis (TG, DSC, TG-FTIR) were applied to investigate thermal stability and behavior of the complexes **1-5**. The results are shown in Figs. S9-S13 in *Supplementary Materials*. The thermal stability of analyzed complexes is comparable - they are stable at room temperature and further heating leads to melting and degradation processes.

Complex **1** decomposes in two step process at about 251 °C and 265 °C (ΔH_1 = 74 kJ kg^{-1} and ΔH_2 = 93 kJ kg^{-1}). Complex **2** decomposes in three step process and begins to decompose at 75 °C, whereas next two steps of degradation occur at 223 and 299 °C (ΔH_1 = 15 kJ kg^{-1}, ΔH_2 = 64 kJ kg^{-1}, ΔH_3 = 55 kJ kg^{-1}). Complex **3** seems to be the most stable one between **1-5** complexes and decompose at 285 °C and then at 390 °C (ΔH_1 = 113 kJ kg^{-1} and ΔH_2 = 14 kJ kg^{-1}). Complexes **4** and **5** begin to decompose at low temperature (75 °C **4** and 102 °C **5**) and degrade in four step process. The subsequent volatilization processes are observed at 227, 258 and 284 °C (ΔH_2 = 2 kJ kg^{-1}, ΔH_3 = 85 kJ kg^{-1}, ΔH_4 = 51 kJ kg^{-1}) for **4** and 164, 223 and 298 °C (ΔH_2 = 2 kJ kg^{-1}, ΔH_3 = 63 kJ kg^{-1}, ΔH_4 = 54 kJ kg^{-1}) for **5**. Melting

point vary insignificantly in the case of **1** complex (246 °C) and notably for **2**-**3** and **5** complexes (196 °C **2**, 253 °C **3**, 205 °C **5**) and occur separately from volatilization processes. After decomposition, a white (**1** and **4**), yellow (**2** and **5**) and black (**3**) powders are obtained as final products.

The progress of decomposition of **1**-**5** complexes was also monitored with the FT-IR spectra (Fig. S14 *Supplementary Materials*). They are similar and show the presence of gaseous products of the decomposition of tri-*tert*-butoxysilyl substituents ($\nu_{(Si–O)}$ = 1074 cm^{-1}, $\nu_{(C–O)}$ = 1193 cm^{-1}). Spectra exhibit also additional bands observed for symmetric and asymmetric scissor-bending vibrations characteristic for tert-butyl residues (1394 and 1371 cm^{-1}) as well as for CH_2 groups present in aliphatic carbon chains of diamines (1477 cm^{-1}) and skeleton vibration of tBu group (1241 cm^{-1}).

4. Conclusions

Considering structures of compounds **1**-**5** it can be said that presented complexes form pentacoordinated complexes of a very similar geometries. The minor structural differences follow the rules observed for other sets of molecular cadmium, zinc and cobalt complexes with sulfur and nitrogen ligands. We have also demonstrated that the thermally stable **1**, **2** and **4**, **5** complexes display luminescent properties which may be essential in future research in design the synthetic candidates for photoactive materials.

Appendix A. Supplementary data

CCDC 826664, 826665, 806104- 806106 contains the supplementary crystallographic data for **1, 2, 3**-**5**. These data can be obtained free of charge via http://www.ccdc.cam.ac.uk/conts/retrieving.html, or from the Cambridge Crystallographic Data Centre, 12 Union Road, Cambridge CB2 1EZ, UK; fax: (+44) 1223-336-033; or e-mail: deposit@ccdc.cam.ac.uk.

Acknowledgement

The Financial support from the Polish Ministry of Science and Higher Education Grant No. N N204 155940 are gratefully acknowledged

References

[1] O. Kahn, Molecular Magnetism, VCH, New York (1997); M.A. Withersby, A.J. Blake, N.R. Champness, P.A. Cooke, P. Hubberstey, W.-S. Li, M. Schrőder, Inorg. Chem. 38 (1999) 2259–2266; G.R. Desiraju, Science 278 (1997) 404–405; J. D. Dunitz, J. Bernstein, Acc. Chem. Res. 28 (1995) 193–200; L. De La Durantaye, T. McCormick, X.-Y. Liu, S. Wang, Dalton Trans. (2006) 5675–5682; X.-J. Chen, Y. Yang, W.-W. He, J.-F. Ma, Polyhedron 65 (2013) 141–151.

[2] B. Kersting, Angew. Chem. Int. Ed. 40 (2001) 3987–3990; J. A. McCleverty, M. D. Ward, Acc. Chem. Res. 31 (1998) 842–851; Y.-B. Huang, G.-R. Tang, G.-Y. Jin, G.-X. Jin, Organometallics, 27 (2008) 259–269; Q. Chen, J. Yu, J. Huang, Organometallics, 26 (2007) 617–625; H. Kwak, S.H. Lee, S.H. Kim, Y.M. Lee, B.K. Park, E.Y. Lee, Y.J. Lee, C. Kim, S.-J. Kim, Y. Kim, Polyhedron 27 (2008) 3484–3492.

[3] P.J. Blower, J.R. Dilworth, Coord. Chem. Rev. 76 (1987) 121–185; I.G. Dance, Polyhedron 5 (1986) 1037–1104; D.T. Corwin, Jr., R. Fikar, S.A. Koch, Inorg. Chem. 26 (1987) 3079–3080; D.T. Corwin, E.S. Gruff, S.A. Koch, Inorg. Chim. Acta 151 (1988) 5–6; S.M. Ostrovsky, K. Falk, J. Pelikan, D.A. Brown, Z. Tomkowicz, W. Haase, Inorg. Chem. 45 (2006) 688–694; A. Dołęga, Coord. Chem. Rev. 254 (2010) 916–937 and references therein.

[4] J.J. Vittal, J.T. Sampanthar, Z. Lu, Inorg. Chim. Acta 343 (2003) 224–230.

[5] S. Jun, E. Jang, Y. Chung, Nanotechnology 17 (2006) 4806–4810; Z. Yang, A.B. Smetana, C.M. Sorensen, K.J. Klabunde, Inorg. Chem. 46 (2007) 2427–2431; L. Cheng, Y. Yuan, X. Zhang, J. Yang, Angew. Chem. Int. Ed. 52 (2013) 9035–9039.

[6] A. Dołęga, K. Baranowska, A. Pladzyk, Acta Crystallogr. Struct. Rep. Online E 63 (2007) m3072; A. Pladzyk, A. Dołęga, K. Baranowska, Acta Crystallogr. Struct. Rep. Online E 63 (2007) m1434–m1436; J. Bąkowicz, A. Kropidłowska, I. Turowska-Tyrk, B. Becker, Acta Crystallogr. Struct. Rep. Online E63 (2007) m973–m975.

[7] A. Pladzyk, K. Baranowska, K. Dziubińska, Ł. Ponikiewski, Polyhedron 50 (2013) 121–130; A. Pladzyk, Ł. Ponikiewski, N. Stanulewicz, Z. Hnatejko, Optical Mat. 36 (2013) 554–561.

[8] A. Pladzyk, K. Baranowska, Z. Anorg. Allg. Chem. 635 (2009) 1638–1644.

[9] A. Dołęga, K. Baranowska, Acta Crystallogr. Struct. Rep. Online E 64 (2008) m616–m617.

[10] R. Piękoś, W. Wojnowski, Z. anorg. allg. Chem. 318 (1962) 212–216.

[11] B. Becker, K. Radacki, W. Wojnowski, J. Organomet. Chem. 521 (1996) 39–49; B. Becker, A. Dołęga, A. Konitz, L. Swinder, W. Wojnowski, Z. anorg. allg. Chem. 627 (2001) 280–286; A. Dołęga, B. Becker, J. Chojnacki, A. Konitz, W. Wojnowski, Inorg. Chim. Acta 357 (2004) 461–467; A. Dołęga, A. Konitz, E. Baum, W. Wojnowski, Acta Crystallogr. Struct. Rep. Online E 61 (2005) m2582–m2584; A. Dołęga, A. Ciborska, J. Chojnacki, M. Walewski, W. Wojnowski, Thermochimica Acta 429 (2005) 103–109; A. Kropidłowska, J. Chojnacki, J. Gołaszewska, B. Becker, Acta Crystallogr. Struct. Rep. Online E 62 (2006) m2260–m2262; A. Dołęga, M. Wieczerzak, K. Baranowska, Acta Crystallogr. Struct. Rep. Online E 63 (2007) m1774; A. Dołęga, A. Pladzyk, K. Baranowska, M. Wieczerzak, Inorg. Chem. Commun. 11 (2008) 847–850; A. Dołęga, K. Baranowska, A. Pladzyk, K. Majcher, Acta Cryst. C 64 (2008) m259–m263; A. Dołęga, A. Pladzyk, K. Baranowska, J. Jezierska, Inorg. Chim. Acta 362 (2009) 5085–5096.

[12] A. Dołęga, J. Chojnacki, A. Konitz, W. Komuda, W. Wojnowski, Acta Crystallogr. Struct. Rep. Online E 62 (2006) m636–m639; A. Dołęga, K. Baranowska, J. Gajda, S. Kaźmierski, M. Potrzebowski, Inorg. Chim. Acta 360 (2007) 2973–2982; A. Dołęga, M. Walewski, Magn. Res. Chem. 45 (2007) 410–415; A. Dołęga, K. Baranowska, Z. Jarząbek, Acta Crystallogr. Struct. Rep. Online E 64 (2008) m1515; K. Baranowska, M. Bulman, A. Dołęga, Acta Crystallogr. Struct. Rep. Online E 68 (2012) m1515.

[13] A. Dołęga, K. Baranowska, D. Gudat, A. Herman, J. Stangret, A. Konitz, M. Śmiechowski, S. Godlewska, Eur. J. Inorg. Chem. (2009) 3644–3660.

[14] A. Dołęga, S. Godlewska, K. Baranowska, Acta Crystallogr. Struct. Rep. Online E 62 (2006) m3567–m3569; A. Pladzyk, K. Baranowska, D. Gudat, S. Godlewska, M. Wieczerzak, J. Chojnacki, M. Bulman, K. Januszewicz, A. Dołęga, Polyhedron 30 (2011) 1191–1200.

[15] C.S. Lai, E.R.T. Tiekink, Cryst. Eng. Comm. 6 (2004) 593–605; C.S. Lai, S. Liu, E.R.T. Tiekink, Cryst. Eng. Commun. 6 (2004) 221–226; D. Chen, C.S. Lai, E.R.T. Tiekink, Cryst. Eng. Comm. 8 (2006) 51–58.

[16] C.S. Lai, E.R.T. Tiekink, Appl. Organometal. Chem. 17 (2003) 251–252; C.S. Lai, E.R.T. Tiekink, Appl. Organometal. Chem. 17 (2003) 253–254; V. Avila, E.R.T. Tiekink, Acta Crystallogr. Struct. Rep. Online E64 (2008) m680; E.R.T. Tiekink, Appl. Organometal. Chem., 22 (2008) 533–550; H.D. Arman, P. Poplaukhin, E.R.T. Tiekink,

Acta Crystallogr. Struct. Rep. Online E65 (2009) m1472–m1473; P. Poplaukhin, E.R.T. Tiekink, Acta Crystallogr. Struct. Rep. Online E65 (2009) m1474; H.D. Arman, P. Poplaukhin, E.R.T. Tiekink, Acta Crystallogr. Struct. Rep. Online E65 (2009) m1475.

[17] S. Liu, J. Zhang, X. Wang, G.-X. Jin, Dalton Trans. (2006) 5225–5230.

[18] J.T. Sampanthar, J.J. Vittal, J. Chem. Soc., Dalton Trans. (1999) 1993–1997.

[19] B. Becker, A. Zalewska, A. Konitz, W. Wojnowski, Z. anorg. allg. Chem. 627 (2001) 271–279.

[20] W. Wojnowski, B. Becker, L. Walz, K. Peters, E.M. Peters, H.G. von Schnering, Polyhedron 11 (1992) 607–612.

[21] G.M. Sheldrick, Acta Crystallogr. A., 64 (2008) 112–122.

[22] A.B.P. Lever, Inorganic Electronic Spectroscopy, second ed., Elsevier Science Publishing Co., Inc., New York, 1984.

[23] A.W. Addison, T.N Rao, J. Reedijk, J. van Rijn, G.C. Verschoor, J. Chem. Soc., Dalton Trans. (1984) 1349–1356; L. Yang, D.R. Powell, R.P. Houser, Dalton Trans. (2007) 955–964.

[24] A. Ciesielski, A.R. Stefankiewicz, M. Wałesa-Chorab, V. Patroniak, M. Kubicki, Z. Hnatejko, J.M. Harrowfield, Supramolecular Chemistry 21 (2009) 48–54.

[25] M.D. Allendorf, C.A. Bauer, R.K. Bhakta, R.J.T. Houk, Chem. Soc. Rev. 38 (2009) 1330–1352.

[26] C.A. Bauer, T.V. Timofeeva, T.B. Settersten, B.D. Patterson, V.H. Liu, B.A. Simmons, M.D. Allendorf, J. Am. Chem. Soc. 129 (2007) 7136–7144.

[27] P.-P. Sun, Q. Chen, X. Zhu, B.-L. Li, H.-Y. Li, Polyhedron 52 (2013) 1009–1015.

[28] S.L. Li, Y.Q. Lan, J.F. Ma, J.Yang, G.H. Wei, L.P. Zhang, Z.M. Su, Cryst. Growth Des. 8 (2008) 675–684.

[29] M. Ahmad, P.K. Bharadwaj, Polyhedron 52 (2013) 1145–1152.

[30] M.Y. Hyun, I.H. Hwang, M.M. Lee, H. Kim, K.B. Kim, C. Kim, H.-Y. Kim, Y. Kim, S.-J. Kim, Polyhedron, 53 (2013) 166–171.

[31] J. Xiang, Y. Luo, L.-L. Zhao, Ch.-H. Wang, J.-S. Wu, Inorg. Chem. Commun. 31, (2013) 23–28.

[32] Y. Wang, Z.-Q. Liu, J.-H. Zhou, T. Wang, S.-N. Wang, G.-X. Liu, X.-X. Wang, Y. Gao, J. Xu, Inorg. Chim. Acta 400 (2013) 169–178.

Supporting figures

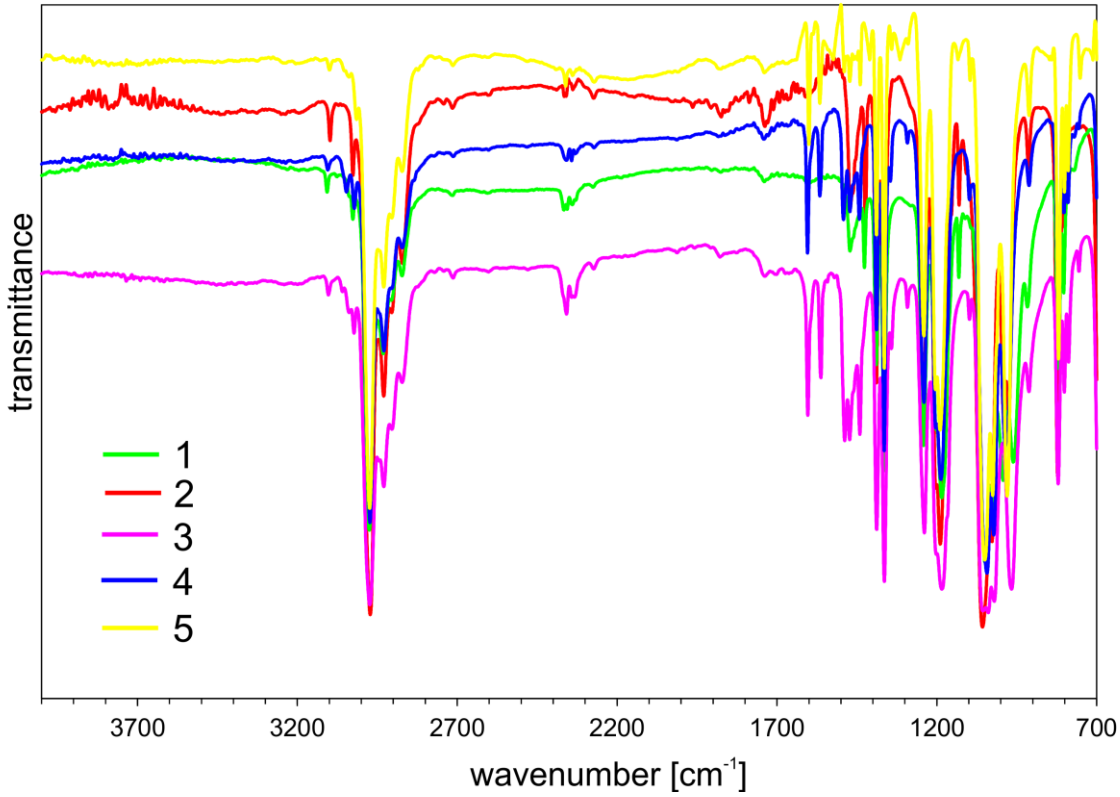

Fig. S1 FT-IR spectra of **1-5** complexes.

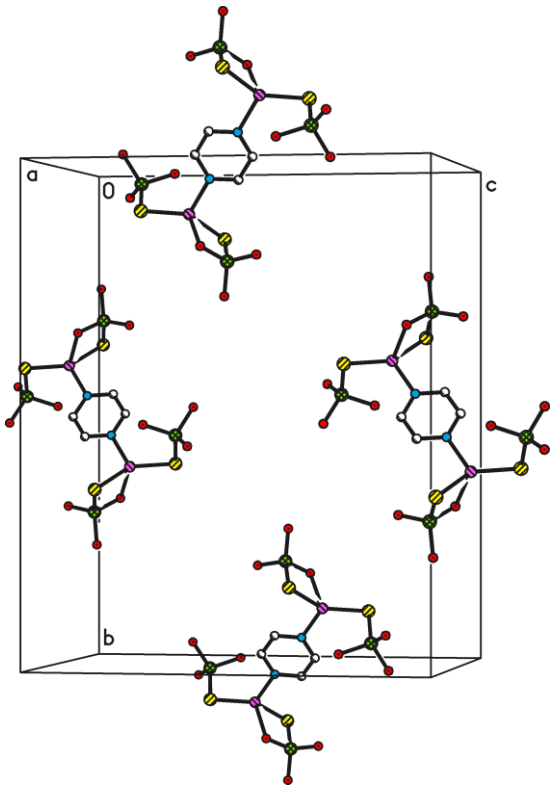

Fig. S2 Crystal packing of **1** along *a* axis. tBu groups and H atoms of aromatic ring omitted for clarity.

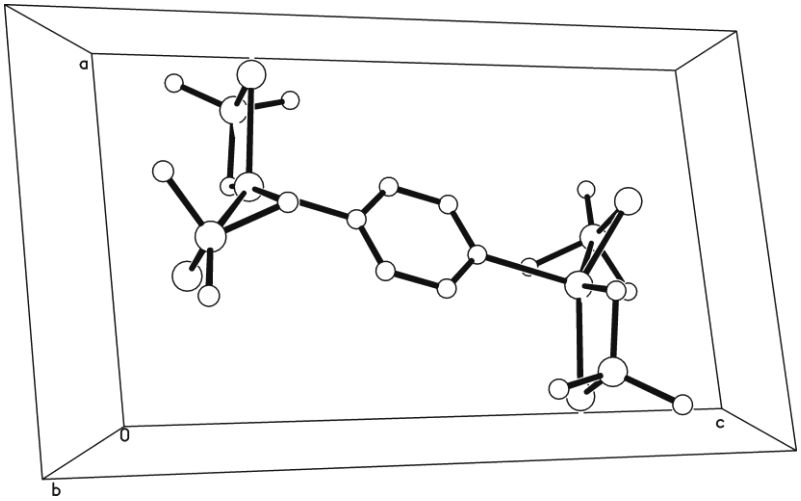

[102] **Fig. S3** Crystal packing of **2** along *b* axis. H atoms of tBuO groups and hydrogen atoms of aromatic rings omitted for clarity.

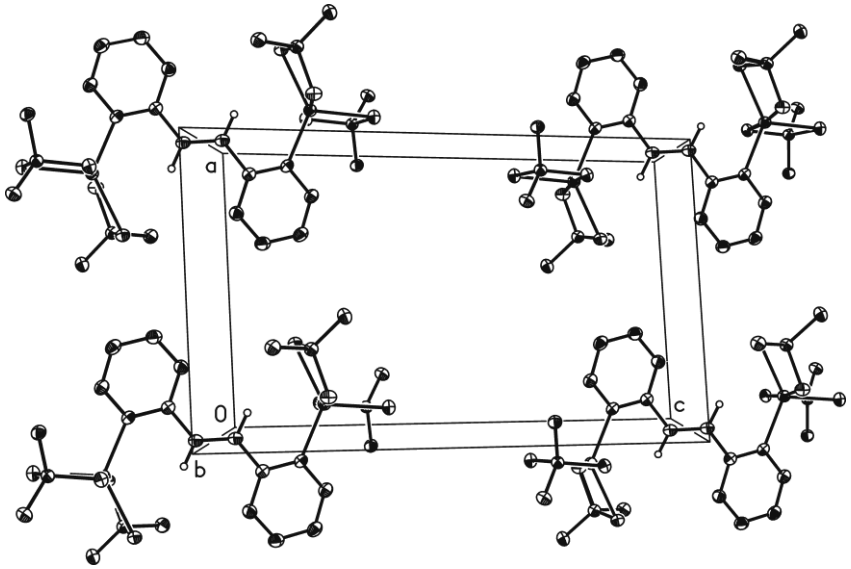

[121] **Fig. S4** Crystal packing of **3** along *b* axis. tBuO groups and hydrogen atoms of aromatic rings omitted for clarity.

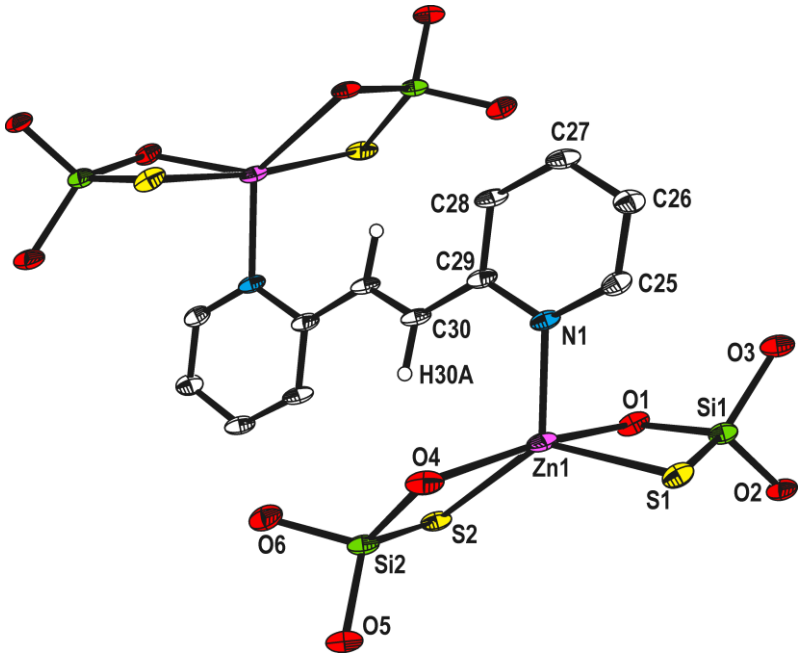

[145] **Fig. S5** Molecular structure of $[Zn_2\{SSi(OtBu)_3\}_4(\mu\text{-}C_{12}H_{10}N_2)]$ **4** with atom labeling scheme (tBu groups and hydrogen atoms of aromatic rings omitted for clarity). Thermal ellipsoids are drawn at 30% probability.

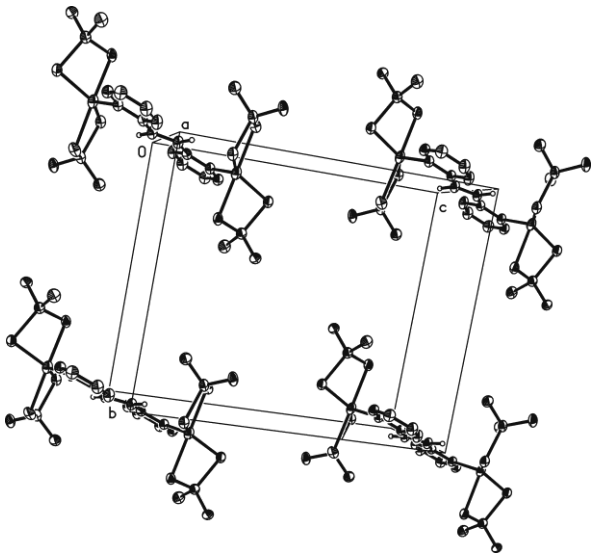

[166] **Fig. S6** Crystal packing of **4** along *a* axis. H atoms of tBuO groups and hydrogen atoms of aromatic rings omitted for clarity.

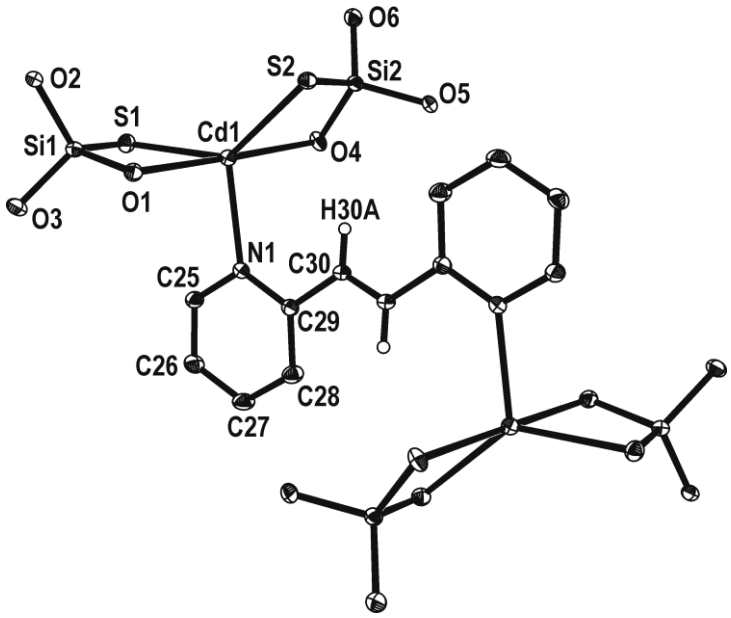

Fig. S7 Molecular structure of $[Cd_2\{SSi(OtBu)_3\}_4(\mu\text{-bpe})]$ **5** with atom labeling scheme (tBu groups and hydrogen atoms of aromatic rings omitted for clarity). Thermal ellipsoids are drawn at 30% probability.

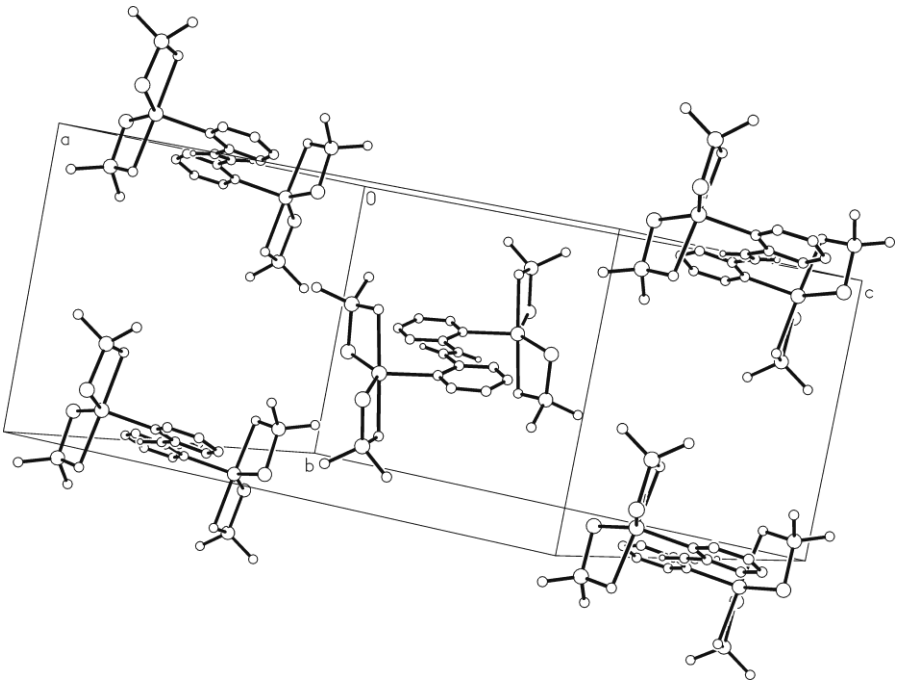

Fig. S8 Crystal packing of **5** along a axis. tBuO groups and hydrogen atoms of aromatic rings omitted for clarity.

[216]

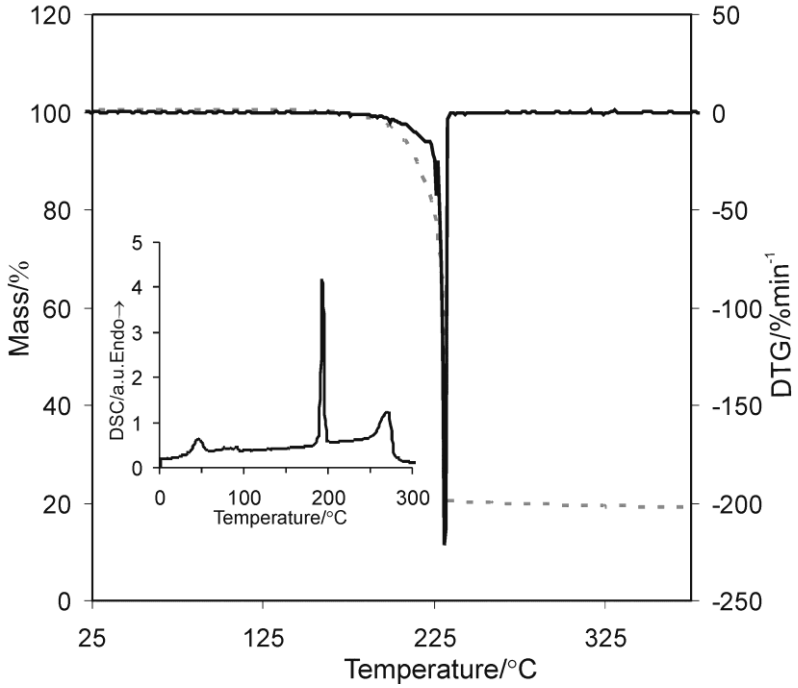

[217]

[218]

[219] **Fig. S9** Thermogravimetric and DSC curves of **1** for the heating rate of 10 K·min^{-1} recorded in dynamic argon atmosphere.

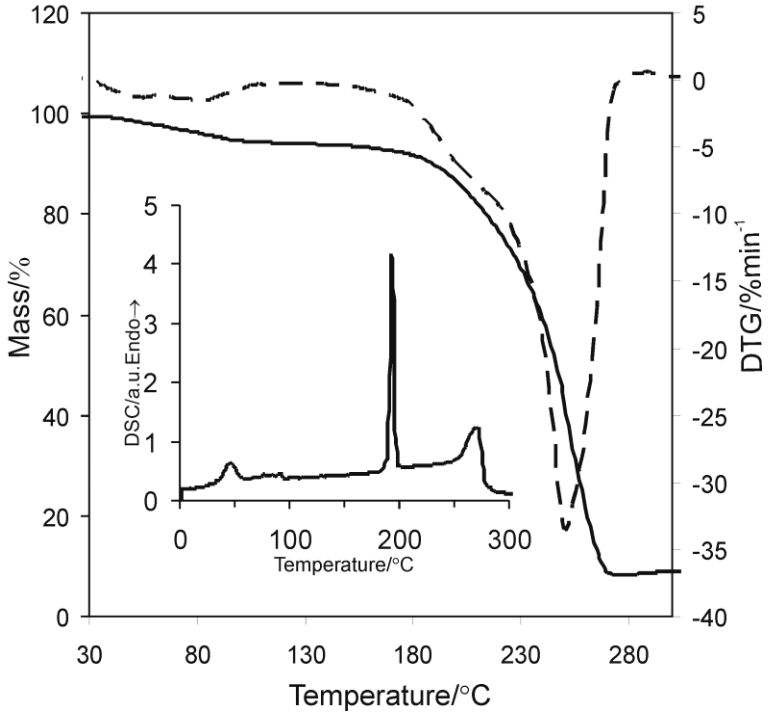

[220]

[221]

[222]

[223] **Fig. S10** Thermogravimetric and DSC curves of **2** for the heating rate of 10 K·min^{-1} recorded in dynamic argon atmosphere.

[224]

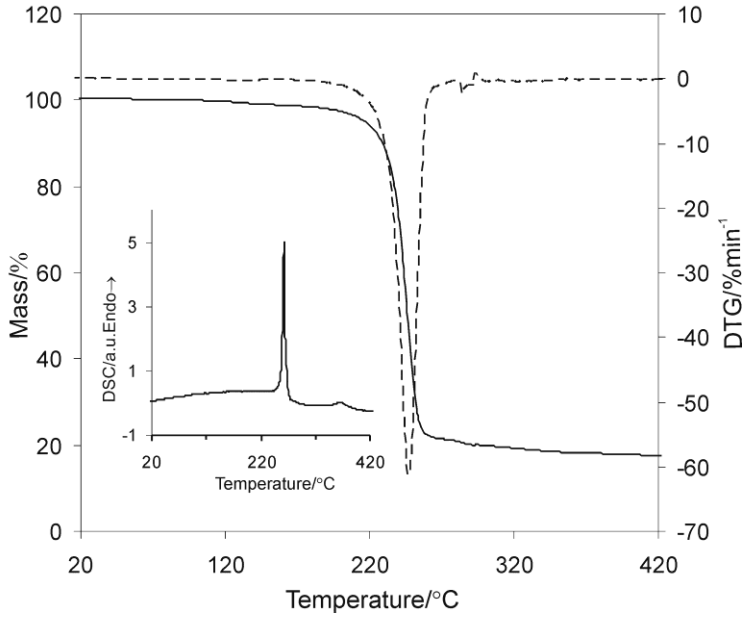

[225] **Fig. S11** Thermogravimetric and DSC curves of **3** for the heating rate of 10 K·min^{-1} recorded in dynamic argon atmosphere.

[226]

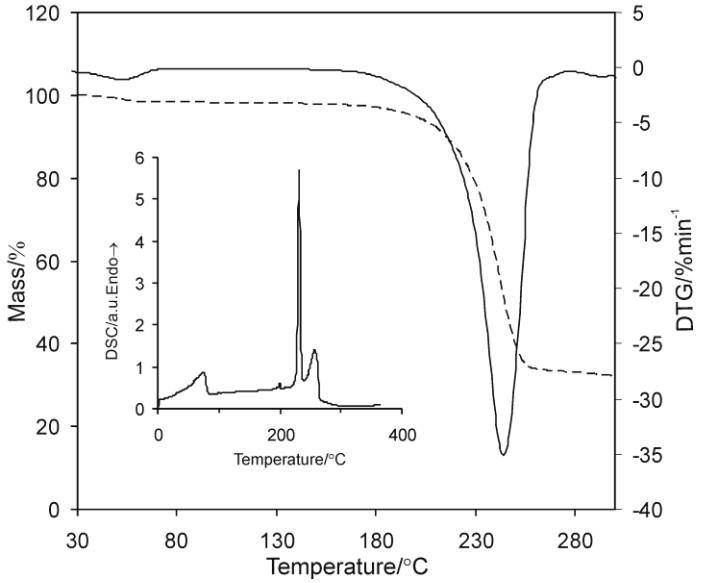

[227] **Fig. S12** Thermogravimetric and DSC curves of **4** for the heating rate of 10 K·min^{-1} recorded in dynamic argon atmosphere.

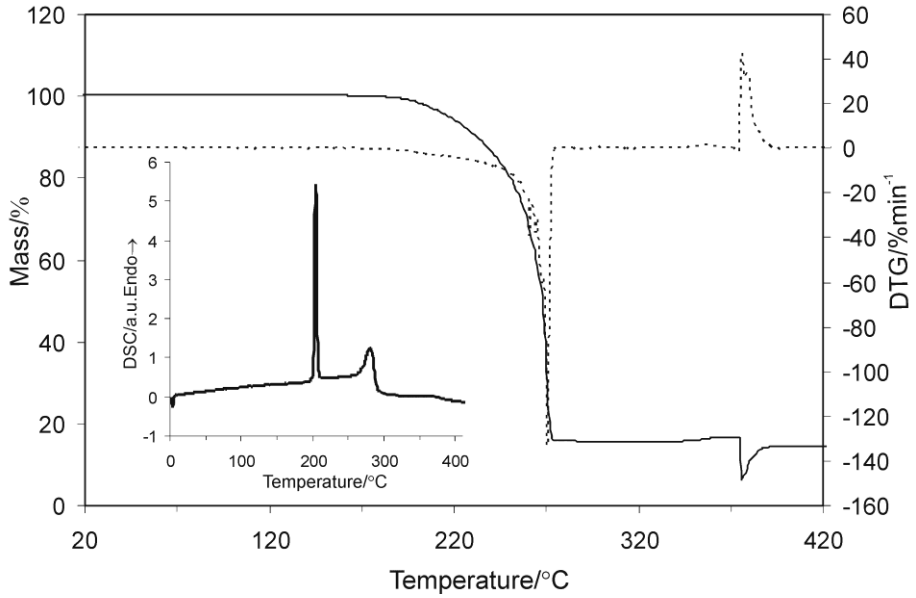

[228] Fig. S13 Thermogravimetric and DSC curves of **5** for the heating rate of 10 K·min^{-1} recorded in dynamic argon atmosphere.

[229]

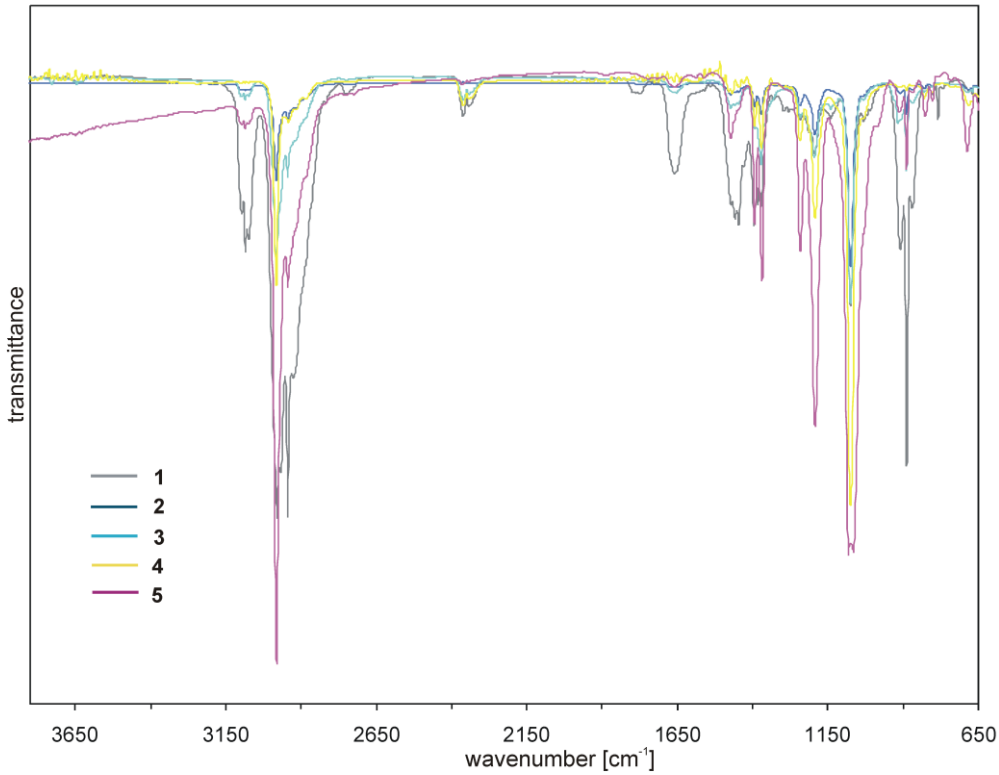

[230]

[231] **Fig. S14** FTIR spectra of the volatiles evolving during TG analysis of **1-5** recorded at 265 °C **1**, 290 °C **2**, 280 °C **3**, 244 °C **4** and 295 °C **5**.

[232]

Table 1. Crystallographic data and structure refinement details

Complexes	**1**	**2**	**3**	**4**	**5**
Empirical formula	$C_{52}H_{112}N_2O_{12}S_4Si_4Zn_2$	$C_{52}H_{112}N_2O_{12}S_4Si_4Cd_2$	$C_{60}H_{118}N_2O_{12}S_4Si_4Co_2$	$C_{60}H_{118}N_2O_{12}S_4Si_4Zn_2$	$C_{60}H_{118}N_2O_{12}S_4Si_4Cd_2$
M_r /g mol^{-1}	1328.78	1422.84	1418.02	1430.9	1524.96
T (K)	120 (2) K	120 (2) K	120 (2) K	120 (2) K	120 (2) K
Wavelength /Å	0.71073 (Mo Kα)	0.71073 (Mo Kα)	0.71073 (Mo Kα)	0.71073 (Mo Kα)	0.71073 (Mo Kα)
Crystal system	monoclinic	triclinic	triclinic	triclinic	monoclinic
Space group	$P2_1/c$	P–1	P–1	P–1	$P2_1/c$
a (Å)	8.6084(3)	9.5944(4)	10.0771(4)	9.7317(3)	17.0227(4)
b (Å)	23.5912(8)	12.5124(7)	12.1055(5)	13.0750(5)	12.2673(3)
c (Å)	18.7859(8)	16.6983(6)	17.1374(6)	15.6893(5)	22.4002(9)
α (°)	90	111.232(4)	107.131(4)	90.077(3)	90
β (°)	104.541(4)	91.896(3)	91.368(3)	92.842(3)	120.061(2)
γ (°)	90	101.133(4)	95.439(4)	96.293(3)	90
V (Å^3)	3692.9(2)	1821.71(14)	1985.87(13)	1981.82(12)	4048.5(2)
Z	2	1	1	1	2
Crystal size (mm)	0.12 x 0.25 x 0.35	0.21 x 0.26 x 0.43	0.38 x 0.18 x 0.09	0.24 x 0.20 x 0.05	0.36 x 0.22 x 0.20
D_{calc} (Mg m^{-3})	1.195	1.297	1.186	1.199	1.251
θ range (°)	2.24 to 25.50	2.41 to 25.50	2.33 to 25.50	2.42 to 25.25	2.68 to 25.25
Reflections collected/unique (R_{int})	14224/6896 (0.0232)	22472/6790 (0.0350)	13394/7399 (0.0318)	11665 / 7048 (0.0229)	14427 / 7322 (0.0235
μ (mm^{-1})	0.877	0.814	0.634	0.822	0.737
Data / restraints / parameters	6896 / 2 / 434	6790 / 0 / 387	7399 / 1 / 401	7048 / 3 / 401	7322 / 0 / 401
Goodness of fit (GOF) on F^2	1.011	1.072	1.096	1.106	1.038
R_1, wR_2 [$I > 2\sigma(I)$]	0.0455, 0.1239	0.0357, 0.0885	0.0467, 0.1422	0.053, 0.1467	0.0357, 0.0887
R_1, wR_2 (all data)	0.0616, 0.1300	0.0437, 0.0926	0.0637, 0.1505	0.0664, 0.153	0.0460, 0.0929
Largest diff. peak and hole (eÅ^{-3})	1.147 and -0.367	1.032 and -0.467	0.720 and -0.585	1.132 and -0.560	1.656 and -0.435
CCDC number	826664	826665	806104	806105	806106

Table 2. Selected interatomic distances (Å) and angles (°) for **1** and **2**.

	1 (M = Zn)	**2** (M = Cd)
Bond lengths		
M(1)–N(1)	2.085(3)	2.392(2)
M(1)–S(1)	2.2578(8)	2.4106(7)
M(1)–S(2)	2.0931(11)	2.4327(7)
M(1)–O(1)	2.271(2)	2.746(2)
M(1)–O(4)	{2.710(2)}	2.5015(19)
Si(1)–S(1)	2.0840(11)	2.0945(10)
Si(2)–S(2)	2.0931(11)	2.0915(10)
Si(1)–O(1)	1.655(2)	1.6562(19)
Si(1)–O(2)	1.618(2)	1.623(2)
Si(1)–O(3)	1.612(2)	1.624(2)
Si(2)–O(4)	1.639(2)	1.6556(19)
Si(2)–O(5)	1.642(2)	1.6146(19)
Si(2)–O(6)	1.606(2)	1.6303(19)
Bond angles		
N(1)–M(1)–S(1)	105.45(7)	111.11(6)
N(1)–M(1)–S(2)	113.48(7)	101.00(6)
S(2)–M(1)–S(1)	140.26(3)	147.75(3)
S(1)–M(1)–O(1)	79.85(5)	69.73(4)
S(1)–M(1)–O(4)	{104.67(5)}	109.73(5)
S(2)–M(1)–O(4)	{72.86(5)}	73.84(5)
S(2)–M(1)–O(1)	105.61(5)	109.73(5)
O(1)–M(1)–O(4)	174.63(7)	171.18(6)
Si(1)–S(1)–M(1)	84.15(3)	87.66(3)
Si(2)–S(2)–M(1)	92.51(4)	86.95(3)

Table 3. Selected interatomic distances (Å) and angles (°) for **3**-**5**.

	3	**4**	**5**
Bond lengths	(M = Co)	(M = Zn)	(M = Cd)
M(1)–N(1)	2.085(3)	1.991(2)	2.329(2)
M(1)–S(1)	2.2916(9)	2.4031(10)	2.4681(7)
M(1)–S(2)	2.2948(10)	2.4782(10)	2.4550(7)
M(1)–O(1)	2.350(2)	2.400(2)	2.5200(18)
M(1)–O(4)	2.340(2)	2.481(3)	2.5282(18)
Si(1)–S(1)	2.0846(13)	2.0634(13)	2.0896(10)
Si(2)–S(2)	2.0817(13)	2.0278(13)	2.0914(10)
Si(1)–O(1)	1.665(2)	1.769(3)	1.6582(19)
Si(1)–O(2)	1.634(2)	1.465(2)	1.6279(19)
Si(1)–O(3)	1.624(3)	1.715(3)	1.6240(19)
Si(2)–O(4)	1.665(2)	1.745(3)	1.6574(19)
Si(2)–O(5)	1.625(2)	1.623(2)	1.6234(19)
Si(2)–O(6)	1.626(2)	1.667(3)	1.621(2)
Bond angles			
N(1)–M(1)–S(1)	130.67(8)	97.83(9)	102.18(5)
N(1)–M(1)–S(2)	108.64(8)	127.57(9)	123.79(5)
S(2)–M(1)–S(1)	120.66(4)	134.56(3)	134.03(2)
S(1)–M(1)–O(1)	76.98(6)	75.79(6)	72.95(4)
S(1)–M(1)–O(4)	97.36(6)	110.22(6)	109.72(5)
S(2)–M(1)–O(4)	78.22(6)	66.83(6)	72.18(4)
O(1)-M(1)-S(2)	102.90(7)	102.09(7)	104.42(4)
O(1)–M(1)–O(4)	174.03(8)	168.75(8)	176.55(6)
Si(1)–S(1)–M(1)	86.59(4)	87.53(4)	86.77(3)
Si(2)–S(2)–M(1)	85.40(4)	96.15(4)	87.99(3)